

NIST

National Institute of Standards and Technology
Technology Administration, United States Department of Commerce

NIST Technical Note 1500-11
Materials Reliability Series

Metallurgy of the U.S. Capitol Dome

T. A. Siewert
C. N. McCowan
J. D. McColskey



*NIST Technical Note 1500-11
Materials Reliability Series*

Weld Repair of the U.S. Capitol Dome

T. A. Siewert
C. N. McCowan
J. D. McColskey

*Materials Reliability Division
Materials Science and Engineering Laboratory
National Institute of Standards and Technology
325 Broadway
Boulder, CO 80305-3328*

A Report to the Office of the Architect of the Capitol on Project
900265 K

December 2002



U.S. DEPARTMENT OF COMMERCE
Donald L. Evans, Secretary

TECHNOLOGY ADMINISTRATION
Phillip J. Bond, Under Secretary for Technology

NATIONAL INSTITUTE OF STANDARDS AND TECHNOLOGY
Arden L. Bement, Jr., Director

National Institute of Standards and Technology Technical Note 1500-11
Natl. Inst. Stand. Technol., Tech. Note 1500-11, 22 pages (December 2002)
CODEN:NTNOEF

U.S. GOVERNMENT PRINTING OFFICE
WASHINGTON: 2002

For sale by the Superintendent of Documents, U.S. Government Printing Office
Internet: bookstore.gpo.gov Phone: (202) 512-1800 Fax: (202) 512-2250
Mail: Stop SSOP, Washington, DC 20402-001

Metallurgy of the U.S. Capitol Dome

T.A. Siewert, C.N. McCowan, and J.D. McColskey
Materials Reliability Division
National Institute of Standards and Technology

This report describes the composition and some properties of the cast iron and wrought iron that form the dome of the U.S. Capitol. It is a compilation of two recent investigations, one by NIST and one by Lucius Pitkin, Inc. These investigations were implemented by the Office of the Architect of the Capitol to determine the dome's condition and also to predict how the outer shell might respond to weld repair of cracks. However, the studies also provide an interesting glimpse into the technology that was in existence at the time of the dome's construction, the mid-1800's, and document (perhaps for the first time) the microstructure and properties of materials that form the dome. Knowledge of the properties and other characteristics of the dome materials is fundamental to maintaining the dome and to predicting its future performance.

Keywords: cast iron; corrosion; fatigue tests; tensile tests; U.S. Capitol dome.

1. Historical Background on the Dome

An understanding of a structure begins with information on its construction and maintenance. A good summary of the construction of the Capitol and its dome is available on the web site of the Office of the Architect of the Capitol [1].

The present dome of the Capitol was built between 1856 and 1866. It replaced an earlier wooden dome that was no longer considered to be in scale with the expansions to the House and Senate wings (expansions needed to accommodate legislators from the states that had just been added to the Union). Cast iron was chosen because it was fire resistant, could be formed in complex shapes, and could be erected with pieces of convenient sizes. The designers also recognized that the dome would be subject to movement due to heating and cooling cycles, and the design included features to accept this movement. The U.S. Capitol Dome was the second cast-iron dome in the world and it remains the largest iron dome to this day.

Although the majority of the dome, particularly its inner and outer shells and lower skirt, is composed of cast iron, wrought iron is used in a few places. The main framing of the dome consists of 36 arched ribs that bear on 36 paired pillars, which in turn, bear on 36 pairs of cast

iron brackets that are embedded in the masonry walls of the Great Rotunda. The ribs are tied together at multiple levels by bands or hoops consisting of either cast-iron sections or wrought-iron riveted plates. From the main rib framing, an elaborate arrangement of cast-iron brackets support the outer shell of the dome and give it its distinctive shape. The inner shell is suspended from the main ribs with either wrought iron hangers or cast iron brackets. Also suspended from the main ribs near the top of the dome is a shell of cast iron grating to which the plaster base of the fresco entitled "The Apotheosis of Washington" is applied. At the top of the dome, the 36 ribs converge into 12 which continue upward to support the Tholos and the Lantern levels, and the Statue of Freedom. These structural parts of the dome were all fabricated in the 1850's and 1860's using the casting technology of the time. More information (including Thomas Walter's elevation and cross-section drawings from 1859) is available at the Office of the Architect of the Capitol web site [1].

Modern structures usually have a steel framework, and many of the components are joined by welding. However, the blast furnace and refining technologies that permitted large-scale production of rolled steel sheets and beams were not introduced until the second half of the 19th century, while welding processes for structural fabrication were not commercialized until the 1930's and 1940's [2]. Therefore, the dome construction in the 1850's was based on the structural metals that dominated before then, cast iron (the most economical) and wrought iron, and was joined by wrought bolts. Cast iron (high-carbon iron that is cast in molds of the desired shapes) is much less common in structures today than it was 140 year ago, because it is inherently more brittle than structural steel, and cannot be shaped by hammering or rolling. Thus, most structures today are constructed of steel. Yet, cast iron is very resistant to thermal shock and damps vibrations. Cast iron is still used in some demanding automotive applications where resistance to heat checking (in brake drums and clutch plates) and vibration (engine cylinder blocks and heavy gearboxes) make it the material of choice.

2. Evaluations of Material in the Dome

In the early 1990's, a study investigating water penetration of the dome during heavy rainstorms revealed problems in several areas, including leakage due to numerous cracks and breaks in the cast iron plates that form the skin of the dome. In turn, the staff from the Office of the Architect of the Capitol sought information on the materials that had been used to construct the dome, as well as advice on how to repair cracks that were found in the skin of the dome. One response came in 1998 from Lucius Pitkin, Inc., an organization with expertise in areas such as mechanical property testing, weld engineering, nondestructive testing, and failure investigations. Their report included an engineering assessment of various structural members comprising the dome [3]. Specifically, this assessment included

- nondestructive characterization of the microstructure and mechanical properties of the ribs and skin of the dome and of the wrought iron tension ring,
- metallurgical testing of samples selected from various structural members, and
- measurement of the thermally induced strains.

Data from their study are included in the next section on results.

During the tour in 1998, we saw that the cast iron rib framework of the dome is in excellent condition. The castings that form the skin have visibly degraded only where corrosion has penetrated the paint (especially where paint could not reach all the surfaces) and has led to rusting, or where the castings that form the skin of the dome have been stressed beyond their ductile limits and have cracked. This led to two studies of possible procedures for weld repair, one in 1998 and one in 2002. A separate report covers the weld procedures and their properties [4]. This report covers the baseline characterization data on the dome materials themselves.

3. Results and Discussion

3.1. Microstructure

Cast irons are iron alloys in which the carbon content exceeds the solubility limit of the austenitic (high-temperature) phase of iron. By definition, cast irons have carbon contents above 2 mass percent, which distinguishes them from the various grades of steel. Besides carbon, alloying elements such as silicon are often added, while impurities can be carried along from the ore or come from the materials added during processing. These other elements have effects as well, however this discussion will concentrate on the carbon. During cooling and solidification, the excess carbon precipitates as either iron carbide or graphite. For the cast irons found in the dome, the excess carbon is found as flakes. This form is known as gray cast iron because the large graphite flakes in the structure give a gray appearance to a fracture surface. Gray iron was very common at the time of the construction of the dome. Since then, many other types of cast iron (ductile, malleable, etc.) have been developed, and are distinguished by the shape of the graphite flakes or nodules [5].

In turn, there are two different classes of gray cast iron in the dome, ferritic cast iron in the ribs and pearlitic cast iron in the skin. Here, the two names refer to the microstructure that surrounds the graphite flakes in the gray cast iron, either a ferritic phase (predominantly iron) or a pearlitic phase (a fine mixture of layers of iron and iron carbide). The ferritic versus pearlitic structure is determined primarily by the cooling rate, with ferritic structure promoted by a slower cooling rate and pearlitic promoted by a faster cooling rate. A secondary reason is that the rib castings have a slightly different composition, the implications of which are discussed in more detail in the following sections. Together, cooling rate and composition explain why a ferritic structure is observed in the massive rib beams, and the pearlitic structure is observed in the thinner skin castings (less than 1 cm thick plates) that form the skin. More information on the distinctions between ferritic and pearlitic iron is included in handbooks on the processing of metals [2, 5-6].

Other structural parts of the dome were constructed of wrought iron, a material produced by mixing molten, high-carbon iron (like cast iron) with oxides. The mixture was "puddled" in a furnace to remove most of the carbon and reduce the concentration of other impurities [2]. The

resulting ball of iron was squeezed into the shape of a bar (to remove excess slag), which could then be rolled into plates or rods. In turn, some rods could be processed into bolts and some plates processed into nuts and washers. The end result was a wide variety of structural components (from plates to nuts) composed of a lower-carbon iron, with layers of silicates, sulphides, and oxides. The tensile strength of the wrought iron is greater than that of gray cast iron, and it is much more ductile. In effect, the additional refining and processing steps added cost, but improved the mechanical properties for use in locations with more demanding requirements. The tension ring at the base of the dome and the bolts and nuts were made from wrought iron.

The report by Lucius Pitkin includes a number of micrographs, some taken from metallurgical specimens and some from replicas taken by polishing the surface of the ribs and plates. None of these micrographs is included here because we only had a photocopy of their report, so the quality of the micrographs was low.

The group from NIST also obtained a few pieces of the dome in 1998, and a few more in 2002, to assist with the two studies of weld repair procedures [4]. These pieces included a few circular coupons removed during the installation of new rain-water drains, and parts of a railing and a gutter that had been replaced in the past. Most of this material was used for the studies of weld repair procedures, but the remaining material further away from the weld (unaffected by the weld thermal cycles) was studied later to obtain data on the original structure. Thanks to the characterization work already done by Lucius Pitkin, NIST was able to concentrate on developing complementary data on the dome materials. Since the dome includes about 4,500 tons of cast iron produced by a number of different foundries during a 10-year period, we tried to evaluate as many pieces as possible to assess the range of compositions and properties likely to occur through the dome.

In the NIST laboratory, we examined several sections of the original skin and confirmed that the microstructure was primarily a pearlitic gray cast iron. The skin castings contained graphite flakes that fit two standard classifications. The castings had a combination of randomly dispersed flake graphite (type A) and graphite rosette (type B) structures, although the microstructure varies from casting to casting and is quite complicated. The type B graphite structure is typical of castings that are cooled more rapidly, such as those with section thicknesses below about 10 mm [5]. Figure 1 shows a region from a skin casting that has both rosettes and randomly oriented flakes between the rosettes. The marker in the lower right of the figure is 200 μm long, so the magnification is about 150 X. This figure is at a relatively low magnification and so is useful in showing the variation in the flake shapes over this section. This micrograph was prepared by grinding a piece of casting on a series of successively finer grits, at each stage removing surface damage introduced by the previous grit. To reveal the internal structure, the final surface was finished by polishing with a fine alumina powder. The black regions are the carbon (graphite) flakes, while the white areas are a mixture of pearlitic and ferritic iron. The type A flakes are the large angular chunks, while the type B flakes are the small clusters of fine flakes (rosettes). Other pieces of castings showed different ratios of the two

graphite structures, varying from solely type A to solely Type B. Such variation in microstructure is not unusual for castings produced over a 10-year period by a number of different foundries, especially when the section thickness is near the transition of type A to type B.

Figures 2 and 3 show regions at magnifications about double that of Figure 1. Figure 2 shows a region with a typical type A structure, while Figure 3 shows one with a typical type B structure. At these higher magnifications, more details of the structure become visible, both variations in the shape of the graphite flakes and slightly different shadings in the areas with the highly reflective surface. The phases in the reflective areas can be better distinguished with the use of an etchant, a chemical solution that reacts at different rates with the various phases. Figure 4 shows the effect of using Klemm's reagent after a nital pre-etch, at a still higher magnification [7-8]. Here, the graphite flakes are still easily distinguished by their acicular shape, while many new phases have become visible. The large, rounded dark areas are pearlite, with fine lines in their interiors marking the alternating layers of iron and iron carbide. The large, rounded light areas are ferrite, so this region would be characterized as a mixed ferrite-pearlite structure, in which the ferrite dominates. The light-colored regions (with small etched islands) at the boundaries of the ferrite and pearlite grains are a low-melting-point eutectic of iron carbide and iron phosphide.

The microstructure serves as a record of how the casting structure developed. As the casting cooled from the liquid, the graphite flakes formed along with austenite (a high temperature phase of solid iron), using up much of the iron, carbon, and silicon in the melt. Finally, the only liquid left had the composition of the low-melting-point eutectic, and filled in the gaps between the austenite grains. Just below the melting temperature, the casting was a mixture of graphite flakes (only a few percent of the volume), austenite (the majority of the volume), and the low-melting-point eutectic (only a few percent filling in the gaps between the austenite grains). As the casting continued to cool, some of the remaining carbon diffused to the carbon flakes and the austenite transformed to a mixture of ferrite and pearlite, determined by the cooling rate and the amount of carbon in the austenite.

With a color camera, even more details are visible. Figure 5 shows a region near that of Figure 4. Here, there are differences in color within the ferrite grains, which indicate a graded change in composition from the center of the grain to the outside. This gradient is known as coring and is quite common in slowly cooled metals. Certain components in the molten metal solidify at slightly higher temperatures. As the liquid is depleted in these components, the layer that is solidifying slowly changes in composition.

Metallography can also help to characterize the structure of the wrought iron plates. Figure 6 shows a cross section through one of the plates, parallel to the rolling direction. Here, the ferrite structure is separated by a multitude of dark horizontal lines, which are slag islands left from the refining process. The slag islands are fairly soft at the rolling temperature and elongated during rolling into these long shapes known as stringers. Figure 7 shows the structure at a higher

magnification. The large stringer in the center fractured into many chunks during the rolling operation, while the smaller stringers stretched elastically. This behavior is due to the variation in composition of individual stringers, including metal sulphides, silicates, and oxides. Of these constituents, some are quite ductile at the rolling temperatures, while other are quite brittle. Figure 8 shows the wrought iron structure with a color etch, similar to that of Figure 5. Here, the ferrite that appeared only as reflective in figures 6 and 7 is revealed to be composed of a large number of smaller grains. This structure explains the good ductility of the wrought iron compared to the cast iron. There are no large graphite flakes to serve as crack starters, and the low level of impurities (such as iron phosphides) means that the ferrite is quite ductile.

3.2. Composition

On one cast iron rib, the team from Lucius Pitkin found the composition (in mass percent) to be 3.39 C, 1.07 Mn, 0.92 Si, 0.61 P, and 0.10 S. On one piece of wrought iron (boiler plate), they found the composition (in mass percent) to be 0.025 C, 0.13 Mn, 0.10 Si, 0.13 P, and 0.01 S. This wrought iron composition matches well with good practice for the production of wrought iron, which was carbon of less than 0.035 mass percent, silicon of 0.075 to 0.15 percent, sulfur of less than 0.02 percent, and phosphorus of 0.1 to 0.25 percent [4]. When composition standards came into use in later years, the U.S. specifications carried a maximum of 0.09 percent Mn, but even then there were exemptions such as “there was no logical ground for condemning an otherwise well-made product because of a relatively high manganese content” [4]. It should also be pointed out that a certain fraction of these elements are incorporated in the slag islands, not in the iron itself. Thus, they have less effect on the mechanical properties of the wrought iron. In other words, a crack in a brittle slag island is less likely to propagate through the wrought iron than a similar crack in a brittle phase in an iron casting.

The group at NIST also measured the composition. Table 1 list the results of spectroscopic analysis of three specimens taken from different castings on the skin of the dome. In addition to the key elements reported by Lucius Pitkin, additional trace elements are listed for one specimen to document the levels of these impurities in the castings in the dome. These compositions can be considered characteristic of the castings produced in this time period. The contents of some key elements differ from those reported by Lucius Pitkin for the rib specimen, but this is not surprising because these castings are from the skin of the dome (and so are predominately pearlitic cast iron rather than the ferritic iron used in the ribs). It seems reasonable to assume that the different foundries produced castings using different formulations, and some adjustments may have been made to the melts to increase the liquidity for the thin skin castings over those for the ribs. For example, the liquidus temperature of a casting drops from 1295 °C to 1175 °C as the carbon content increases from 2.5 to 3.6 mass percent [5]. If the maximum temperatures in the furnaces were limited by the technology of the time, dropping the liquidus temperature by adding carbon would have been the easiest way to increase the superheat of the casting (the temperature difference between the melt and that of solidification) and so increase the ability of the liquid metal to fill the furthest corners of the mold. In addition, lower temperatures greatly

reduce the damage to the mold during pouring of the iron, so increased carbon content is the best way to combine a complete fill of a thin mold with a good surface appearance. This reasoning further explains the higher carbon content in the skin castings.

Incidentally, the skin castings do have periodic rough areas on the inner surfaces that may mark where risers were removed during cleaning of the castings. Riser is the casting term for a reservoir of liquid metal used to feed metal into the casting to offset solidification shrinkage. Only in a few places, such as changes in section size, did we find solidification shrinkage in the castings. One of these locations, beneath a tab on a railing section, is shown in figure 9.

Table 1. Composition of pearlitic gray cast iron from the skin of the dome.

| Element | Specimen 1 (mass %) | Specimen 2 (mass %) | Specimen 3 (mass %) |
|-------------------|------------------------|------------------------|------------------------|
| C | 3.36 | 3.62 | 3.86 |
| Mn | 0.67 | 0.82 | 0.48 |
| Si | 3.20 | 2.18 | 2.31 |
| P | 0.78 | 0.82 | 0.60 |
| S | 0.11 | 0.08 | 0.06 |
| Cr | | | 0.01 |
| Ni | | | 0.04 |
| Mo | | | 0.01 |
| Cu | | | 0.02 |
| Al | | | 0.001 |
| Ti | | | 0.11 |
| Carbon equivalent | 4.7 | 4.62 | 4.83 |

Table 1 also includes a value for carbon equivalence (CE), a term used here to characterize the behavior of cast iron as being above or below the eutectic composition (4.3 mass percent C) on the iron-carbon phase diagram. While many different formulas have been developed to compute the carbon equivalence, one common and simple version is

$$CE = C + (Si + P)/3, \tag{1}$$

where the elements are in mass percent [9]. This equation for carbon equivalence indicates that

both silicon and phosphorus function like carbon in determining the microstructure, but at one-third its effectiveness. The cast iron composition (from a rib, as reported by Lucius Pitkin) had a CE of 3.9, well below that of the eutectic composition (and so known as hypoeutectic), while the cast iron from the skin had CEs from 4.62 to 4.83, well above that of the eutectic composition (and so known as hypereutectic). This difference in carbon equivalent also suggests differences in the structures between the rib and skin castings.

Note that this CE combines the relative effect of the various components in the cast iron on the solidification mode. There are other CEs that calculate the relative effect of the various components in the cast iron on the crack resistance during reheating, such as when the casting might be heated prior to repair by welding.

Modern gray cast irons usually have carbon contents between 2.5 and 4 mass percent and silicon contents between 1 and 3 mass percent [9]. Being at the high end of the range for both elements (also having a high P content) means that the carbon equivalents for the dome castings are unusually high. However, the high carbon equivalent is not the goal by itself, but it is rather a by-product of aiming to make the cast iron more fluid and to promote a gray cast iron structure in such a thin-wall casting. Solidification of a composition with a lower carbon content in such a thin section could favor the formation of a white iron structure, one even more brittle than gray iron [5].

While the carbon is the most important variable in cast irons, other elements have roles as well. Silicon promotes the formation of the carbon flakes and improves the corrosion resistance, and so is kept in the range of 1 to 3 mass percent. Phosphorus does not have a desirable effect for this application and is present only because it was carried along from the ore and refining operations.

3.3. Mechanical Properties

The group from Lucius Pitkin used a few 12 mm (1/2 in) square or round tensile specimens to determine that the ferritic iron castings (dome ribs) had tensile strengths of between 120 and 130 MPa (17.4 and 18.8 ksi), while the wrought iron had a tensile strength near 325 MPa (46 ksi). These values are typical of the materials produced at the time. To minimize the amount of material that they needed to remove from the dome, they evaluated several more ferritic and pearlitic castings using a Brinnell hardness tester, and then converted these values to equivalent strengths. For seven different cast ribs (ferritic structure), they measured hardnesses of 130 to 160 BHN, which correspond to strengths of 110 to 165 MPa (16 to 24 ksi), in close agreement with the strength measurements. For three exterior cast plates (pearlitic) in the dome, they measured hardnesses of 158 to 179 BHN, which correspond to tensile strengths of 158 to 186 MPa (23 to 27 ksi), slightly higher than those obtained from tensile tests on the ferritic cast irons. All the casting strengths are lower than those of most current-technology gray iron castings, which usually have strength minimums of 210 to 280 MPa (30 or 40 ksi), although there are

grades as low as 140 MPa (20 ksi) and as high as 420 MPa (60 ksi). The strength is determined by factors such as the composition and cooling rate.

The group at NIST made several measurements of the tensile strength of the pearlitic cast iron from a piece of the gutter. The width of the gutter, about 115 mm, determined the length of the tensile specimens, and resulted in reduced-section specimens such as those shown in Figure 10. Other than in length and the use of clamp rather than pin grips, the specimens were machined to the sheet-type specimen dimensions shown in Figure 1 “Rectangular Tension Test Specimens” of ASTM Standard E 8 “Standard Test Methods for Tension Testing of Metallic Materials” [10]. The faces of the specimens were machined enough to remove the surface damage, and so had final thicknesses near 7 mm, which were just under the original thickness of the casting. The specimen width was machined to 12.5 mm, producing a cross-sectional areas near 90 mm². Because of the low ductility expected for cast irons, the elongation was measured by strain gages bonded to the machined faces, as shown in Figure 11. The data from the tensile tests were developed following the procedures in E 8, and are listed in Table 2.

Table 2. Tensile test data.

| Specimen | Ultimate Strength (MPa) | Ultimate Strength (ksi) | Elastic Strain at Fracture (%) | Plastic Strain at Fracture (%) |
|------------|-------------------------|-------------------------|--------------------------------|--------------------------------|
| BM-1 | 186 | 27 | 0.18 | 0.25 |
| BM-2 front | 182 | 26.4 | 0.25 | 0.19 |
| BM-2 back | 183 | 26.5 | 0.25 | 0.19 |
| BM-3 front | 168 | 24.5 | 0.22 | 0.17 |
| BM-3 back | 170 | 24.6 | 0.19 | 0.18 |

The dual-displacement-strain measurements per specimen (front and back) were designed to detect any bending, after the relatively low elongation value was observed in BM-1. Any bending would have a relatively large effect on the measurement of small elongations such as those for the cast iron, but the almost exact correspondence between the data for the fronts and backs of the other specimens confirms that little bending occurred.

These tensile strength data compare well with the values calculated by Lucius Pitkin from the hardness measurements. The strength measurements also compare well with predictions based on compositions and microstructure. The high carbon equivalent that helped to increase the fluidity during the casting operation negatively affected the strength. Increasing the carbon equivalent from 3.5 to 4.5 in gray iron castings lowers the tensile strength from about 350 MPa to 150 MPa [5]. Thus the low strength (compared to typical gray iron castings today) can be attributed partially to the high carbon equivalent, which can be attributed in turn to the practical aspects of foundry technology of the time. It reflects the balance between the desire to gain fluidity while keeping the melting temperature low.

No yield strengths are reported for the skin specimens because all specimens failed before or just after meeting the 0.2 percent offset plastic criterion of E 8. However, the strain gages provided an accurate measure of the actual plastic deformation to failure, which ranged from 0.17 to 0.25 percent. The plastic strain did not appear suddenly after a period of elastic loading, but occurred gradually and progressively as the load was applied. Figure 12 shows the record of a typical stress-strain test. Here, the stress is shown along the vertical scale and the strain along the horizontal scale. The record begins at no load or strain, in the lower left of the figure, and continues to failure of the specimen in the upper right. A tangent is drawn parallel to the first part of the record to estimate the slope of the curve during the elastic loading. The curve begins to deviate from this straight line at a very low load, perhaps as low as 25 MPa (4 ksi). Thus, tensile damage begins to accumulate at very low stresses (about 20 percent of the ultimate strength), and confirms that the dome is very sensitive to slight bending or tensile loads, such as occur when the corrosion products build up in the joints. Several unloading cycles during the tensile tests provided a rough estimate of the modulus, around 83 GPa, somewhat lower than the handbook value of near 100 GPa [11]. Tensile loading is an unusual condition for most of the dome. Most of the structure is designed to be in compression. We did one uniaxial test in compression and measured an ultimate strength of about 540 MPa (77 ksi) and a strain of about 1.6 percent. These values are only approximate, because the specimen started to buckle at this point, making further analysis very complicated. The real message is that the cast iron is about twice as strong in compression as in tension, and it has greater elongation.

The group at Lucius Pitkin did not calculate yield or elastic strains for the rib specimens, but the chart records included in their report allow rough estimates of these properties to be made [2]. The strain curves for two rib specimens begin to deviate from pure elastic behavior at about 40 MPa (6 ksi), a value similar to that for the skin castings. The curves reach stresses of about 100 MPa and 120 MPa (15 and 17 ksi) at a plastic strain of 0.2 percent (the traditional definition of yielding), then continue to stretch to final elongations of 0.3 and almost 0.5 percent. The rib castings are distinctly more ductile than the skin castings.

Gray cast irons are typically stronger by a factor of two in compression than in tension, supported both by the single test of skin material and literature [9]. Thus, the tensile values quoted in the table above can be nearly doubled for modeling of compression applications. The application of cast iron for compression members and wrought iron for tension members indicates a recognition of these characteristics by the designers of the dome, and helps to explain its good performance over the years.

The curvature of the tensile test data (figure 12) suggested that plastic deformation begins at low loads and strains. To get a better understanding of the development of this damage, we prepared several more specimens like those used for the tensile tests, and exposed them to cyclic loads (fatigue tests). We used a servohydraulic test machine to apply a sinusoidal load spectrum. We clamped the ends of the specimens, then cycled between a minimum and maximum tensile load. Based on the low cyclic loads (mostly thermal expansion) on the dome, we started with a load just above the first deviation from elastic behavior in figure 12 (about 25 MPa or 4 ksi), a load

thought to represent the intensity of variable loads on the dome due to snow, wind, and thermal cycles. We then cycled between this load and half this load until fracture (an R ratio of 0.5). Table 3 shows the data from these tests.

Table 3. Fatigue tests on skin material.

| Maximum Load (MPa) | Minimum Load (MPa) | Cycles to Failure |
|--------------------|--------------------|-------------------|
| 35 | 17.5 | > 180,000 |
| 70 | 35 | > 180,000 |
| 105 | 52.5 | 60,000 |
| 105 | 52.5 | > 180,000 |
| 140 | 70 | > 180,000 |

Table 3 shows some quite encouraging results from the fatigue tests. Below maximum tensile loads of 105 MPa (15 ksi), the fatigue specimens were still intact and crack-free up to 180,000 cycles. The tests were terminated after this value because it corresponds to almost 500 years of daily thermal cycles (caused by the usual day to night temperature swings and the heating of the sun as it passes over the surface of the dome). Since the dome has experienced only about one third of this life, there should be ample remaining life for loads at this level. In addition, most of the loads on the dome are expected to be compressive, so these tensile test results would be conservative estimates of compression fatigue behavior. Only once at 105 MPa, did we note a fracture, and then only after 60,000 cycles. This failure initiated at a 2 mm deep corrosion pit on the surface of the specimen. Additional specimens at 105 MPa and at 140 MPa were still intact and free of cracks up to 180,000 cycles. Other than the one failure at a maximum load of 105 MPa after 60,000 cycles at a preexisting corrosion pit, all specimens lasted 180,000 cycles at maximum loads up to 140 MPa.

The group at Lucius Pitkin also calculated the equivalent stresses (based on modulus) of thermally induced strains to be +4.3 to -9.4 MPa (+630 to -1360 psi) over a temperature range of 17 °C (30 °F). Even when expanded to cover the maximum temperature fluctuation from summer to winter, the thermally induced stresses are only a small fraction of the tensile strength of the cast iron or wrought iron. However, their report does not mention whether the strain gage data were corrected for thermal effects.

4. Summary (based on evaluation of specimens taken from the dome)

The rib castings

- are gray iron with a type A (random) distribution of graphite flakes,
- have a ferritic structure around the graphite flakes because their massive sections limited

the cooling rate. The slow cooling rate is further supported by the large size of the graphite flakes, some near 0.8 mm long, and

- have yield strengths near 110 MPa, tensile strengths near 130 MPa, and elongations between 0.3 and 0.5 percent.

The skin castings

- are gray iron with a combination of type A (random) and type B (rosette cluster) distributions of graphite flakes,
- have a mixture of pearlitic and ferritic grains around the graphite flakes because their thinner section promoted faster cooling. The faster cooling rate is further supported by the smaller graphite flakes, usually below 0.2 mm long, and
- fracture at strengths near 180 MPa, but at elongations of only about 0.18 percent, not quite reaching the traditional criteria for a yield strength. However, this characteristic is not unusual, since yield strength is not required and seldom even measured for cast irons [5]. Only where the corrosion products have built up in the joints between castings, have there been any failures of the castings.
- can handle fatigue loads of 70 MPa (10 ksi) at an R value of 0.5 for a lifetime beyond 180,000 cycles.

The tension ring and plates

- are wrought iron, typical of that produced in the 19th century,
- have a ferritic structure with long stringers of non-metallic inclusions (slag), and
- have ultimate strengths near 325 MPa (46 ksi).

5. References

- [1] http://aoc.gov/projects/dome_ren/dome_ren_overview.htm [November 2002]
- [2] *The Making, Shaping, and Treating of Steel*, 9th Edition, U.S. Steel, Herbeck and Held Publishers, Pittsburgh, 1971, pp. 8 to 28.
- [3] *United States Capitol Dome Structural Member Assessment - Washington, D.C.*, Lucius Pitkin, Inc. Report M98028, July 14, 1998.
- [4] T.A. Siewert, C.N. McCowan, R.A. Bushey, J. Doherty, T. Christ, D.J. Kotecki, D.L. Olsen, L.W. Myers, Jr., E. Hinshaw, and S. Kiser, *Weld Repair of the U.S. Capitol Dome*, NIST TechNote 1500-10, 2002.
- [5] *Properties and Selection: Irons, Steels, and High-Performance Alloys, Metals Handbook, Tenth Edition, Volume 1*, ASM International, Materials Park, Ohio, 1990, pp. 3 to 32.
- [6] R. Bushey, "Welding of Cast Irons," chapter in *Welding, Brazing, and Soldering, Metals*

Handbook, Tenth Edition, Volume 6, ASM International, Materials Park, Ohio, 1993, pp. 708 to 721.

- [7] “Metallographic Techniques for Cast Irons,” chapter in *Metallography, Structures and Phase Diagrams, Metals Handbook, Eighth Edition, Volume 8*, ASM International, Materials Park, Ohio, 1973, p. 92.
- [8] G. Vander Voort, *Metallography: Principles and Practice*, McGraw Hill, 1984, p. 642.
- [9] *Properties and Selection: Irons, Steels, and High-Performance Alloys, Metals Handbook, Ninth Edition, Volume 1*, ASM International, Materials Park, Ohio, 1990, p. 4.
- [10] “Standard Test Methods for Tension Testing of Metallic Materials,” ASTM Standard E 8, *Annual Book of ASTM Standards 2002, Vol 3.01*, ASTM International, Philadelphia, Penn., 2002.
- [11] *Smithells Metals Reference Book, Sixth Edition*, Butterworths, 1983, . 15-2.



Figure 1. A micrograph of a skin casting, showing a combination of graphite rosettes and randomly oriented flakes. The marker in the lower right is 200 μm long, so the magnification is about 150 X.



Figure 2. A region of a casting with a type A graphite structure (300 X).

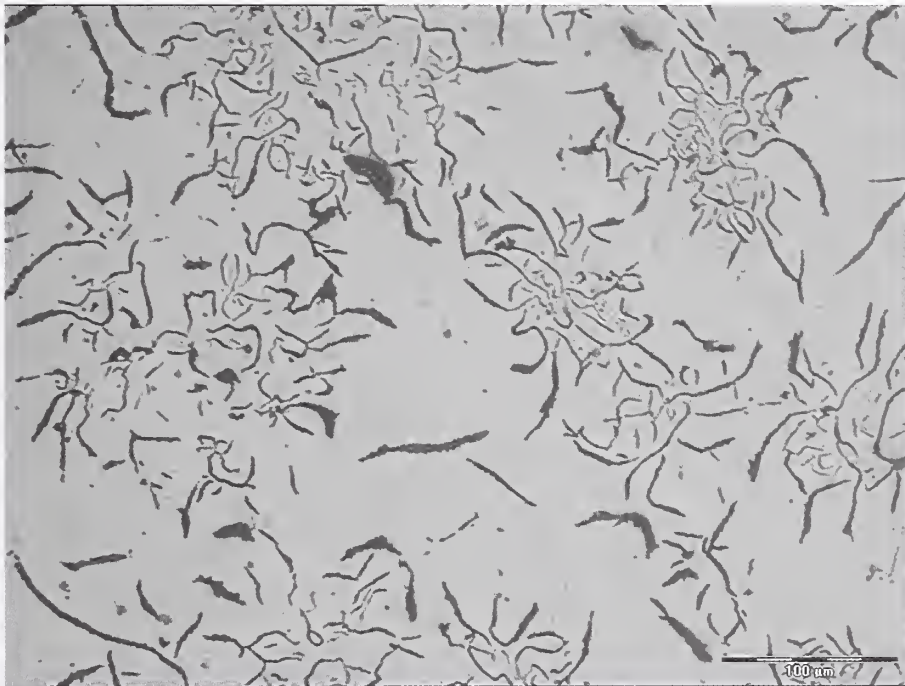


Figure 3. A region of a casting with a type B graphite structure (300 X).



Figure 4. Section of casting etched to show phases present in the areas that appeared white on the earlier figures. Approximate magnification 600 X.

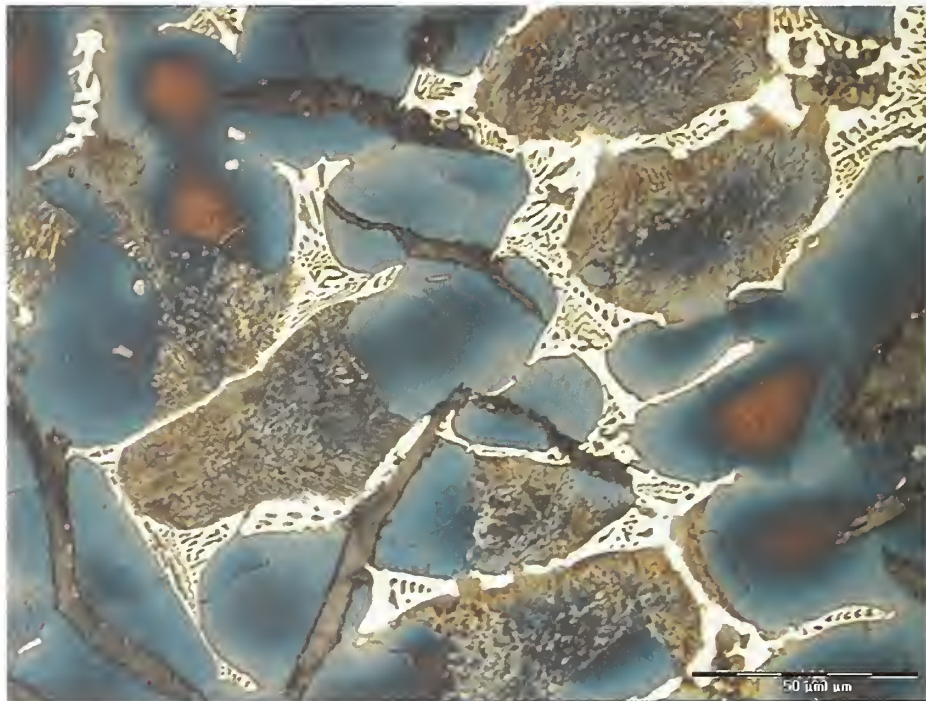


Figure 5. Color etching of an area similar to that of Figure 4, emphasizing the phases.



Figure 6. Cross section through a wrought iron plate. About 60 X.

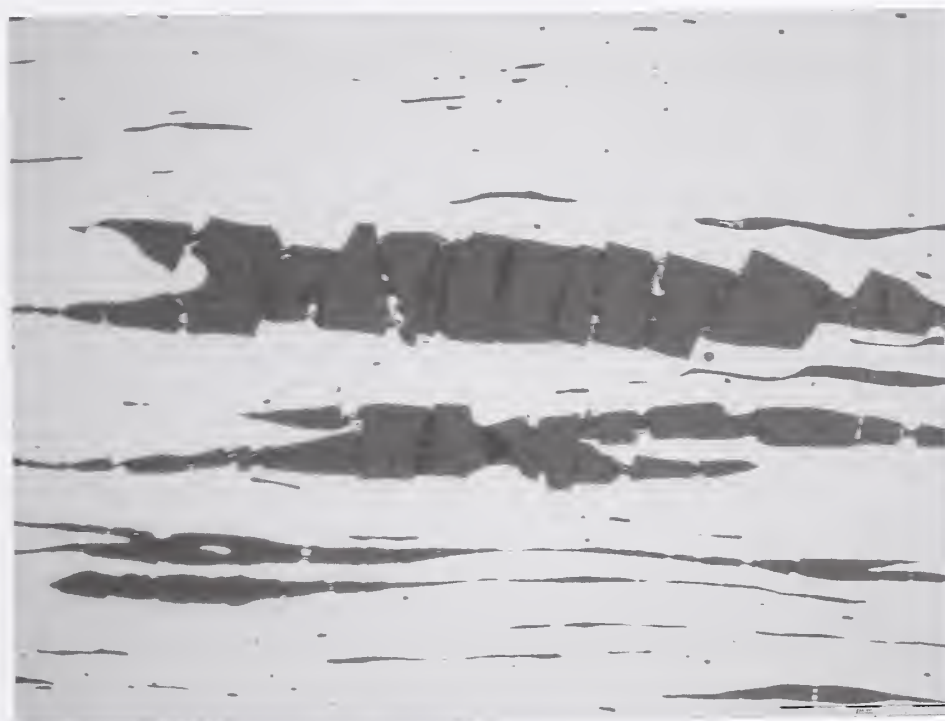


Figure 7. Higher-magnification view of wrought iron structure (400 X).

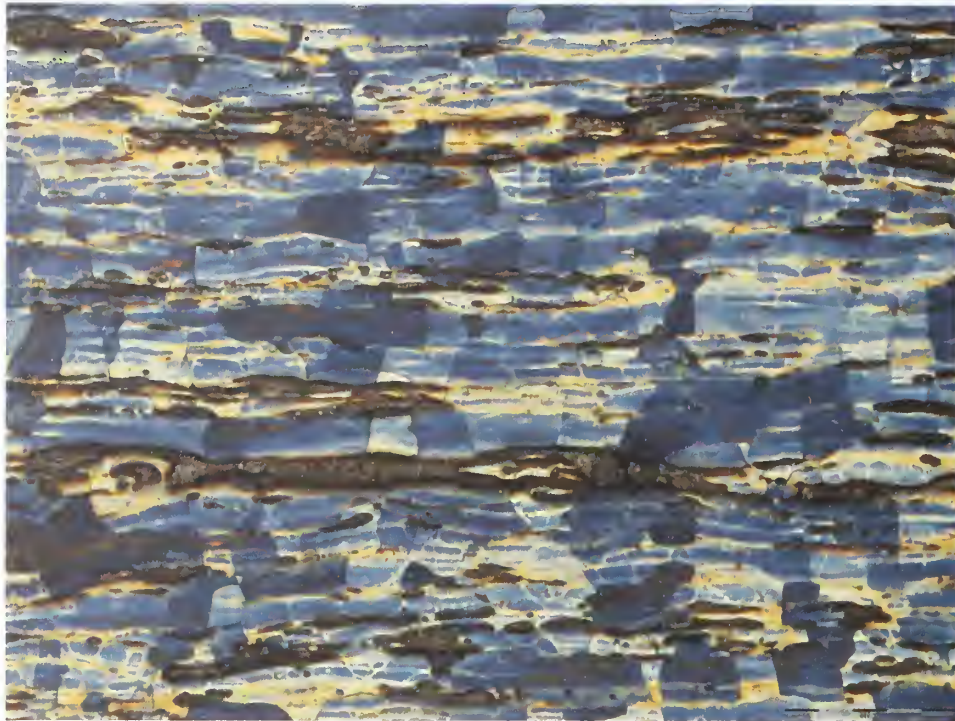


Figure 8. Color etch of an area similar to figure 7 showing the ferrite grains. (150 X)



Figure 9. Low-magnification image of an internal pore discovered during sectioning through a tab in a railing section (10 X).



Figure 10 Reduced-section tensile specimens machined from dome material.

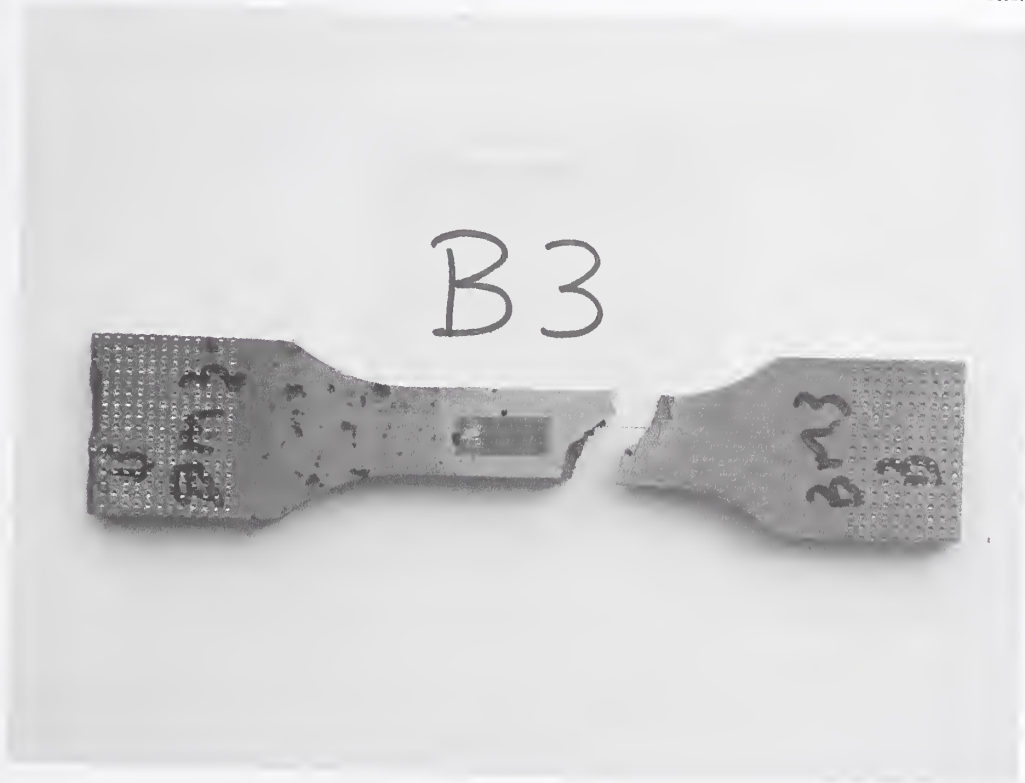


Figure 11. Representative fracture of gray cast iron, specimen BM-3.

Capital Dome Tensile BM-1

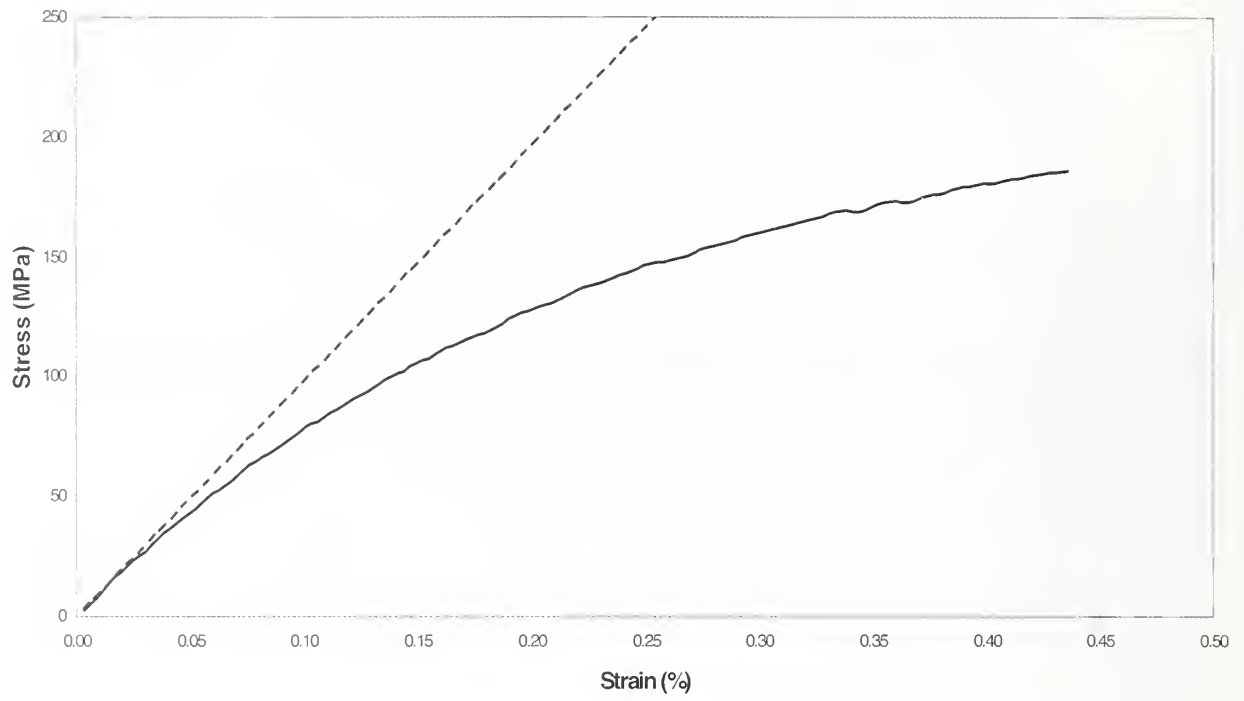


Figure 12. Stress-strain curve for specimen BM-1.

NIST Technical Publications

Periodical

Journal of Research of the National Institute of Standards and Technology—Reports NIST research and development in metrology and related fields of physical science, engineering, applied mathematics, statistics, biotechnology, and information technology. Papers cover a broad range of subjects, with major emphasis on measurement methodology and the basic technology underlying standardization. Also included from time to time are survey articles on topics closely related to the Institute's technical and scientific programs. Issued six times a year.

Nonperiodicals

Monographs—Major contributions to the technical literature on various subjects related to the Institute's scientific and technical activities.

Handbooks—Recommended codes of engineering and industrial practice (including safety codes) developed in cooperation with interested industries, professional organizations, and regulatory bodies.

Special Publications—Include proceedings of conferences sponsored by NIST, NIST annual reports, and other special publications appropriate to this grouping such as wall charts, pocket cards, and bibliographies.

National Standard Reference Data Series—Provides quantitative data on the physical and chemical properties of materials, compiled from the world's literature and critically evaluated. Developed under a worldwide program coordinated by NIST under the authority of the National Standard Data Act (Public Law 90-396). NOTE: The Journal of Physical and Chemical Reference Data (JPCRD) is published bi-monthly for NIST by the American Institute of Physics (AIP). Subscription orders and renewals are available from AIP, P.O. Box 503284, St. Louis, MO 63150-3284.

Building Science Series—Disseminates technical information developed at the Institute on building materials, components, systems, and whole structures. The series presents research results, test methods, and performance criteria related to the structural and environmental functions and the durability and safety characteristics of building elements and systems.

Technical Notes—Studies or reports which are complete in themselves but restrictive in their treatment of a subject. Analogous to monographs but not so comprehensive in scope or definitive in treatment of the subject area. Often serve as a vehicle for final reports of work performed at NIST under the sponsorship of other government agencies.

Voluntary Product Standards—Developed under procedures published by the Department of Commerce in Part 10, Title 15, of the Code of Federal Regulations. The standards establish nationally recognized requirements for products, and provide all concerned interests with a basis for common understanding of the characteristics of the products. NIST administers this program in support of the efforts of private-sector standardizing organizations.

Order the above NIST publications from: Superintendent of Documents, Government Printing Office, Washington, DC 20402 or <http://bookstore.gpo.gov/>.

Order the following NIST publications—FIPS and NISTIRs—from the National Technical Information Service, Springfield, VA 22161 or <http://www.ntis.gov/products>.

Federal Information Processing Standards Publications (FIPS PUB)—Publications in this series collectively constitute the Federal Information Processing Standards Register. The Register serves as the official source of information in the Federal Government regarding standards issued by NIST pursuant to the Federal Property and Administrative Services Act of 1949 as amended, Public Law 89-306 (79 Stat. 1127), and as implemented by Executive Order 11717 (38 FR 12315, dated May 11, 1973) and Part 6 of Title 15 CFR (Code of Federal Regulations).

NIST Interagency or Internal Reports (NISTIR)—A special series of interim or final reports on work performed by NIST for outside sponsors (both government and nongovernment). In general, initial distribution is handled by the sponsor; public distribution is by the National Technical Information Service, Springfield, VA 22161 or <http://bookstore.gpo.gov/index.html>, in hard copy, electronic media, or microfiche form. NISTIR's may also report results of NIST projects of transitory or limited interest, including those that will be published subsequently in more comprehensive form.

U.S. Department of Commerce
National Institute of Standards and Technology
325 Broadway
Boulder, Colorado 80305-3337

Official Business
Penalty for Private Use, \$300